Answers to comments of Review #1

We gratefully thank the reviewers for the positive feedback on our submitted manuscript. We appreciate the time they took to extensively read and comment on the given manuscript. The constructive comments are very helpful for the improvement of the manuscript. Our replies to the referees' comments are structured as follows:
Referee's comments in italic – line numbers according to initially submitted manuscript
Authors' responses in roman – line numbers according to adjusted manuscript. **Citations from the initial and the adjusted manuscript are given in bold.**

In some places the authors seem to discuss findings which are not too surprising and well known. In these places discussion could be slightly shortened and additional literature could be referenced. This is the case in the discussion of the sunglint shape and the Cox and Munk parameterization as well as the impact of "horizontal photon transport".

We considered this valid suggestion and revised some parts of the manuscript. Details to these changes are given in the replies to the specific comments below:

- The shortening of the discussion of the Cox and Munk parametrization is addressed in the answer to comment on line 245.
- The discussion of the horizontal photon transport is shortened drastically, especially for the separated sea ice HDRF. The shortening followed the comment from Referee #2 on lines 310f.

Abstract: Please state somewhere in the abstract that this is a case study for one SZA and a 20-minute data set. For some time, I expected more after reading the abstract.

We agree, that our study is very limited to this one 20 min case, which should be addressed already in the abstract. We changed the respective sentence: "**Therefore, in this case study, an averaged hemispherical-directional reflectance factor (HDRF) of the inhomogeneous surface (mixture of sea ice and open ocea) in the MIZ is derived using airborne measurements collected with a digital fish-eye camera during a 20 minute low-level flight leg in cloud-free conditions.**" (l. 6–9)

l.45 – Please name the difference between BRDF and HDRF. BRDF – direct illumination only. HRDF – including diffuse light.

Yes, this came to short in the original manuscript. We added the following sentence making clear the different nature of the incident radiation (direct/diffuse): "**While the BRDF only considers direct illumination from one single direction, also diffuse illumination from the entire hemisphere is taken into account by the HDRF.**" (l. 46ff.). Later, we give a more detailed introduction to the quantities in Sect. 2.1. For further details we refer in this section to literature (Nicodemus et al., 1977, Schaepman-Strub et al., 2006).

L62 and l.63 – “goniometer” should be “spectrogoniometer” or “goniospectrometer”. Otherwise, it is just for measuring angles.

Thanks for your comment. I was not aware of that and changed it accordingly in l. 66 and 67.

Eq.3 – Why did you omit the "d" in “dFi” e.g.? It is still incremental in i and r, isn'it?

Since the incident irradiance originates from the entire atmosphere (at least the diffuse component) for the HDRF, F_i isn’t an infinitesimal quantity anymore. The reflected radiances, however, are still infinitesimal quantities, since, in the proper definition of the HDRF, the radiation is reflected into infinitesimal solid angles. However, infinitesimal quantities cannot be measured. Strictly speaking, we derive a hemispherical-conical reflectance factor. However, as the solid angle of the camera pixels are rather narrow, we refer to the quantity derived from the measurements as HDRF, which is commonly done in literature.

To make this more clear, we adjusted the text (l. 102–113):

“**Since the illumination under atmospheric conditions is a combination of a direct and a hemispherical diffuse irradiance component with the fractions f_{dir} and $f_{diff} = 1 - f_{dir}$, respectively, both BRDF and BRF cannot be measured practically. Therefore, the hemispherical-directional reflectance factor (HDRF, dimensionless) R_{HDRF} is introduced (e. g., Schaepman-Strub et al., 2006):**

(updated equation 3): $\boldsymbol{R_{\mathrm{HDRF}}(\theta_{\mathrm{i}},\varphi_{\mathrm{i}},2\pi,\theta_{\mathrm{r}},\varphi_{\mathrm{r}}) = R_{\mathrm{BRF}}(\theta_{\mathrm{i}},\varphi_{\mathrm{i}},\theta_{\mathrm{r}},\varphi_{\mathrm{r}})\cdot f_{\mathrm{dir}} + R(2\pi,\theta_{\mathrm{r}},\varphi_{\mathrm{r}})\cdot f_{\mathrm{diff}}}$

The reflectance factor of the diffuse radiation incident over the entire hemisphere is denoted by $R(2\pi;\vartheta_r,\varphi_r)$, were 2π refers to the diffuse radiation incidence. The direction of the direct component is given by ϑ_i and φ_i. The spectral dependence is omitted here. If the diffuse fraction of the incident radiation is sufficiently small, the HDRF represents a good approximation of the BRF. Since the infinitesimal quantities in Eqs. 1–3 are not measurable, in practice, measurement optics with sufficiently small opening angles are applied to approximate the finite radiances. Thus, from a measurement perspective, the HDRF is obtained by:

(new equation 4): $\boldsymbol{R_{\mathrm{HDRF}}(\theta_{\mathrm{i}},\varphi_{\mathrm{i}},2\pi,\theta_{\mathrm{r}},\varphi_{\mathrm{r}}) = \frac{\pi\ \mathrm{sr}\cdot I(\theta_{\mathrm{i}},\varphi_{\mathrm{i}},2\pi,\theta_{\mathrm{r}},\varphi_{\mathrm{r}})}{F(\theta_{\mathrm{i}},\varphi_{\mathrm{i}},2\pi)}}$

To be consistent, we also changed equation 2 and added $\boldsymbol{f_{\mathrm{BRDF,id}}}$ after “**constant BRDF of a Lambertian surface**” (l. 99):

new equation 2: $\boldsymbol{R_{\mathrm{BRF}}(\theta_{\mathrm{i}},\varphi_{\mathrm{i}},\theta_{\mathrm{r}},\varphi_{\mathrm{r}}) = \frac{f_{\mathrm{BRDF}}(\theta_{\mathrm{i}},\varphi_{\mathrm{i}},\theta_{\mathrm{r}},\varphi_{\mathrm{r}})}{f_{\mathrm{BRDF,id}}} = \pi\ \mathrm{sr}\cdot f_{\mathrm{BRDF}}(\theta_{\mathrm{i}},\varphi_{\mathrm{i}},\theta_{\mathrm{r}},\varphi_{\mathrm{r}})}$

l.151 – “inter-calibrated”. With which instrument? Obviously SMART, but please state it.

True. For clarity, we added “**with SMART**” at the end of the sentence (l. 159f).

l.156 - Why does error propagation of two relative errors around 4% for the quotient HDRF not lead to the sum of relative errors 8% as textbooks teach? Please explain your derivation in the manuscript.

We applied the rules of the Gaussian error propagation, which resulted in a total uncertainty of about 6 %. We clarified that by changing the sentence to: “**Thus, using the Gaussian error propagation, the total uncertainty of the calculated HDRF amounts to about 6 %.**” (l. 167f)

l.159 – Please add the original publication “Mayer and Kylling” to the reference here.

Done. (l. 169)

l.180: Please extend c = Ired/Iblue = 0.95 here.

We added that (l. 192). Additionally, we defined the variables in one of the previous sentences: “**Secondly, a color ratio defined by the ratio of the radiances measured in the red (I_{red}) and the blue (I_{blue}) camera channel…**” (l. 190ff).

Fig. 3 – There is “sunglint” around all ice edges? And “sea ice” around the sunglint? How relevant is this? How large is the error? Please discuss.

The impression that the ice edges are classified as sunglint results only from a poor rendering of the color map while plotting. We fixed this issue and revised Fig. 3b, which now shows much less missclassified pixel around the ice edges. The remaining misclassifications are not avoidable with such a simple sea ice mask.

The misclassification of sunglint as "sea ice" is not easy to remove. Obviously the information content of the three wavelength channels is not sufficient to distinguish the margin of the sun glint area from sea ice. However, the number of pixel affected by this misclassification is still low compared to the entire image. Thus, this misclassification is within the uncertainty range of the sea ice fraction. Since the separated sea ice HDRF does not show any offset in these particular viewing angles, the impact of the missclassification is concluded to be negligible. The effect on the separated open ocean HDRF should be limited to the sunglint margins, where the variability is high anyways. This makes us confident, that the misclassification does not have a significant effect on the following data analysis and interpretation.

We added this discussion in the revised manuscript: “**Figure 3b illustrates the surface types identified by the sea ice mask. Together, both panels show the capability of the simple approach to separate between the surface types. Misclassifications mainly affect pixels at the sunglint margin (misclassified as sea ice), which do not have significant implications on the discussion and interpretation in this study. The uncertainty of the sea ice fraction due to the limitations of the sea ice mask is analyzed in the following section. The complete decision process of the sea ice mask is summarized in Fig. 4.**” (l. 193–199)

Fig. 5 – It would be interesting to see variations of this distribution for changes in thresholds as discussed in the text. Think about adding them.

We revised Fig. 5 and added three additional distributions, representing the lowest and the highest sea ice fractions to get an impression of the distribution and the change of the sea ice fractions. However, since the distribution with the lowest sea ice fraction has significantly more misclassifications of sea ice as sunglint, it was not considered in the analysis of the uncertainty range of the mean sea ice fraction. Thus, also the second-lowest distribution is plotted in the new Fig. 5. To describe the new figure, we adapted the text slightly:

"**The frequency distribution of the derived sea ice fraction is shown in black in Fig. 5 shows. Images with higher sea ice fractions were more frequent than images dominated by open ocean. The dashed line indicates the mean sea ice fraction of 0.83 sampled during the 20-minutes measurement time interval. The accuracy of the sea ice fraction depends on the choice of the thresholds that are applied in the sea ice mask. In order to estimate the uncertainty related to the choice of the HDRF threshold values, a sensitivity study was performed, slightly varying one of the thresholds while the others were held constant. Two additional distributions, representing the lowest and the highest resulting sea ice fraction, are illustrated in Fig. 5.**

The thresholds h_1 and h_2 were varied between the two modes (0.2 to 0.6). Changing h_1 or h_2 by 0.1 leads to a change in sea ice fraction of about 1.2 %. h_3 and the color ratio threshold c were varied between 1.2 and 1.4, and 0.9 and 1.0, respectively. The sensitivity to the sea ice fraction is higher, when h_3 or c are decreased. However, the lower limits of both h_3 and c were chosen such that the amount of obvious misclassification of sea ice as sunglint is limited. As visible in Fig. 5, the averaged sea ice fraction resulting from the variation of the thresholds ranges between 0.79 and 0.86. Thus, the uncertainty of the sea ice fraction due to the sea ice mask is estimated to be less than 4 %." (l. 205–217)

The caption of Fig. 5 is changed to "**Frequency distribution of the sea ice fraction resulting from the applied sea ice mask for all images taken within the 20-minute time interval (black) and for adapted sea ice masks (color-coded). The vertical dashed lines represent the resulting mean sea ice fraction.**"

Updated Fig. 5: **Frequency distribution of the sea ice fraction resulting from the applied sea ice mask for all images taken within the 20-minute time interval (black) and for adapted sea ice masks (color-coded). The vertical dashed lines represent the resulting mean sea ice fraction.**

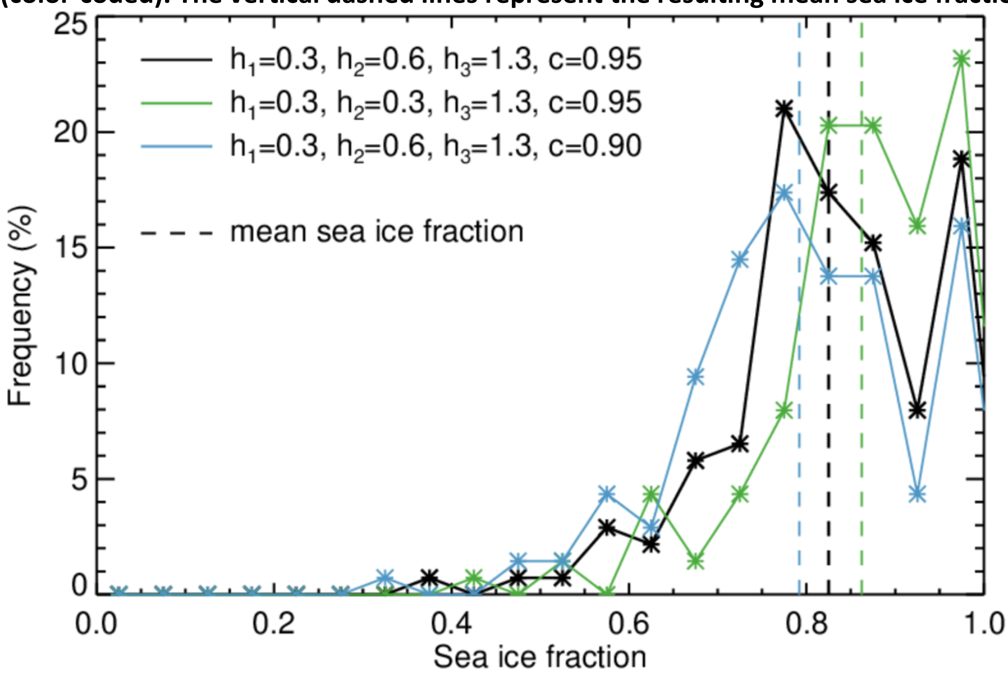

l.215 – A standard deviation of 0.6 for a basis value of 0.11 is really large. Please discuss.

The standard deviation of 0.6 for a basis value of 0.11 is indeed quite high. We identified misclassifications of sea ice pixels as sunglint (which are assigned to open ocean) as the reason for that, which are not easy to remove with our simple mask. However, the mean value is not heavily affected. We clarified that in the text, also giving the standard deviation if the sunglint criteria (thresholds h_3 and c) would not have been applied. Additionally, we shortened the discussion of the variability due to the low number of open ocean observations since we concluded that this is not the contribution to the variability of the open ocean HDRF. We adjusted the discussion on that: "**The standard deviation (blue shading in Fig. 6b) is up to 0.6 outside the sunglint and up to 9.2 in the sunglint region. The high standard deviation outside the sunglint results from misclassifications of sea ice as "sunglint" which are, thus, assigned to open ocean. For each direction, the fraction of open ocean pixels classified as sunglint (calculated as ratio of all images) is referred to as pixel-based sunglint fraction and indicated by the grey line in Fig. 6b. Even on the shadow side, about 10% of the pixels are contributions of misclassified sunglint. Neglecting the sunglint criteria (h_3 and c) would prevent from these misclassifications and reduce the standard deviation to 0.11. Additionally, some of the observed variability results from the high sea ice fraction, which leads to a low number of open ocean pixels in the entire data set. Although the pixel-based sea ice fraction (black line in Fig. 6b), which is derived similarly to the pixel-based sunglint fraction, is higher than 0.8 for most reflection directions, it also reveals significant directional variability.**" (l. 231–239)

The earlier introduction of the pixel-based sunglint fraction then requires slight changes in the following paragraph: "**The irregular shape of the sunglint is likely a result of the low number of observations and is imprinted in the pixel-based sunglint fraction.**" (l. 242f).

The discussion of the different reasons for the HDRF variability required changes in the comparison of open ocean and sea ice HDRF (Sect. 4.2): "**The maximum standard deviation below 0.2 reveals a lower variability compared to open ocean (0.6, including the misclassifications), which indicates that the mean sea ice HRDF is less affected by misclassified pixels.**" (l. 291ff).

Fig.6 – What about white lines in the dark part of the image?

You mean the lines at the top of the image? These are gaps, where open ocean observations were not available within our dataset. They are close to the edge of the image, where, depending on the heading/attitude of the aircraft, not every image delivers data. By changing the color code of the figure, these gaps are now less visible.

Fig.6 – The figure b is quite confusing at a first glance (while it is understandable reading the related paragraphs in the main text). Please add some more details to the caption. Questions that pop up without it: How can sea ice fraction be a function of reflection angle? How can sunglint fraction and sea ice fraction add up to more than 1?

You are right. That could be confusing. We tried to solve this problem by rephrasing the respective sentence "**The black line denotes the mean pixel-based sea ice fraction (the portion of images, where the respective pixel of the solar principle plane is assigned to sea ice). The grey line denotes the mean pixel-based sunglint fraction (the ratio of the number of images, where the respective**

pixel of the solar principle plane is classified as sunglint to the number of images, where this pixel is assigned to open ocean)." Hopefully, that's more clear now.

l.245 and l.249 - "already … 2002" does sound awkward here, as it is obviously correctly considered in the Cox and Munk publication which was based on observations as well. The impact of "reflected skylight" and the need to remove it for their parameterization is discussed there. Please mention.

We agree that "already 2002" sounds odd. However, I wonder why the simulations of Su et al. (2002) didn't capture the sunglint shift, although they used the Cox & Munk slope distribution. Anyway, also regarding your general command, we reduced the discussion about the open ocean HDRF theory by rephrasing the respective paragraph:

"**Cross-sections of the simulated open ocean HDRF for several wind speeds are shown in Fig. 7. For low wind speeds, two local maxima of the open ocean HDRF are visible, representing the sunglint (around the specular point) and the reflection of the diffuse incident radiation towards the horizon. With increasing wind speed, the sunglint distribution becomes broader, while its maximum decreases in intensity and is shifted further to the horizon (e. g., Su et al., 2002). The HDRF peak at the horizon increases with increasing wind speed, which is likely due to an increase of diffuse incident radiation caused by multiple scattering between sea surface and atmosphere. For wind speeds higher than about 3.5 m s^{-1}, the diffuse reflection peak becomes dominant while the sunglint vanishes in its slope. The impact of the diffuse radiation (reflected skylight) on the BRDF and a method to remove this offset were discussed by Cox and Munk (1954).**" (l. 261–268)

L256 – Maybe 0.5 m/s - if you could have simulated it - would have provided an even better match.

Sure. We think so, too. However, simulations with lower wind speed were not supported by libRadtran. That's what we also meant with "**(or even less)**". Of course, the wind speed which would fit best to our observations, remains unclear. We added the sentence "**Unfortunately, simulations with lower wind speeds were not supported by libRadtran.**" (l. 273f) to further clarify this.

l.261 – Do you have "large SZA"? 60 deg doesn't sound too large. Apart from that I have the impression that your results with all their additional uncertainties regarding mix of ice fractions, limited accuracy of glint identification, and true vs effective wind speeds are not suited to analyze the limitations of a theoretical parameterization (Cox and Munk). You could shorten this a bit.

That's true, although we didn't have the intention to evaluate the parametrization of Cox & Munk. Rather, we wanted to discuss the discrepancy of our measured HDRF compared to the simulated one. You are correct that our limited data set could be responsible for the deviations. However, the SZA of 60° present in our observations is relatively large compared to the observations used by Cox & Munk (their SZA was max. 35°). We wanted to note, that similar discrepancies were observed earlier, without claiming the total correctness of one of the studies. We tried to clarify that by adjusting our wording: "**The remaining discrepancy in maximum HDRF between observation and simulation (1 ms^{-1}) could be due to the limited data set (e. g., the variability of the sunglint shape) or the still too high wind speed. However, since similar differences for high SZAs have been observed by Su et al. (2002), this might also be an effect of the larger SZA compared to the original measurements by Cox and Munk (1954).**" (l. 276–279) *l.285/286 – This seems like a quasi-constant offset because of the nearby dark open ocean influence. Please state this here.*

It was remarked by Referee #2 that, given an open ocean fraction of 17 % and a change of the separated water HDRF of 0.09 due to possible 3D effects, the opposite effects on the 83 % sea ice cannot explain an offset of 0.1 to 0.2. Thus, these effects should only be minor for sea ice. Instead, we argue that the our HDRF (partly snow-covered ice floes) lies between the HDRF of fully snow-covered surfaces and bare ice (which fits with Fig. 9). We revised the last two paragraphs of the section completely (see below). We refer to the reply on the comment by Referee #2 lines 310f.

L296 – "However, the optical …" - Why "however"? I was confused first. I was expecting a snow grain size for Goyens, but got one for Carlsen. Please check wording and improve if possible.

Since the argumentation with snow grain size is misleading given that our observed ice surfaces are only partly snow-covered, we revised the last two paragraphs of the section completely (see below).

l.311 – "horizontal photon transport mentioned above" – I agree, but why not putting this into clearer words. "the nearby dark ocean surface", "the reduced diffuse light due to the nearby dark ocean" …

As stated above, we spend less attention to the impact of the nearby ocean surface in our revised text. However, one remark on that is still included (see below).

Revised paragraphs:

"**Compared to the separated sea ice HDRF (black line), the snow HDRF from Carlsen et al. (2020) has a similar shape, but shows a higher magnitude for all reflection directions of the solar principle plane (0.19 at nadir). Likewise, the HDRF of snow-covered sea ice (yellow line) observed by Goyens et al. (2018) is larger than the separated sea ice HDRF (0.16 at nadir), except for reflection zenith angles less than –60°. However, comparing both snow HDRFs, significant differences in their anisotropies are obvious. While the anisotropy of the snow HDRF measured by Carlsen et al. (2020) is lower than that of the separated sea ice HDRF (the difference between both reduces to 0.12 at 59°), the anisotropy is significantly larger for the snow-covered sea ice HDRF (Goyens et al., 2018) with a maximum difference to the separated sea ice HDRF of 0.95 at 77°. In contrast to the other HDRF distributions with a minimum in nadir viewing direction, the minimum of the snow-covered sea ice HDRF by Goyens et al. (2018) is located in backward direction (at about –60°). The reasons for the anisotropy differences of both snow HDRFs (Carlsen et al., 2020, Goyens et al., 2018) remain unclear and might result from, e. g., snow grain size, impurity load or surface roughness. While the measurements from Carlsen et al. (2020) were at a wavelength 538 nm (green channel), the HDRF at 628 nm (red channel) by Goyens et al (2018) were used for comparison. However, the spectral dependence of the snow HDRF in the spectral range is small. The increased variability of the snow-covered sea ice HDRF observed by Goyens et al. (2018) might be due to the smaller footprint of the ground-based measurements compared to the airborne observations. In particular, small-scale surface roughness features can be resolved, which contribute to the variability of the**

ground-based measurements. In contrast to the snow-covered surfaces, the HDRF of bare ice (brown line) is significantly lower than the separated HDRF of the airborne observations and is characterized by an increased anisotropy. This is most prominent at reflection zenith angles of about 60°. However, the shape of the bare ice HDRF distribution is less smooth and shows a variability, that is even larger than that of the snow-covered sea ice HDRF. According to Goyens et al. (2018), this is due to the presence of thawed ice nearby highly reflective ice grains, which often occurs at the beginning of the melt season.

The magnitude of the separated sea ice HDRF analyzed in this study ranges between the literature values for snow-covered and bare ice HDRF. This is reasonable since the observed ice floes revealed a mixture of snow-covered and bare ice (e. g., Fig. 1c). The comparison of the different HDRFs illustrates the variability of the snow and sea ice HDRF in polar environments, which is affected by a variety of properties (e. g., snow cover, snow grain size or impurity concentration). Due to the significantly larger area fraction of sea ice compared to open ocean, the impact of the nearby darker open ocean surfaces in terms of horizontal photon transport should be much smaller (< 0.02) for sea ice and can, thus, not completely explain the differences between the analyzed HDRFs." (l. 302–328)

l.355 – I do not understand what you neglect here? The sea ice fraction is central part of Fig.10c and not neglected. Please adjust wording.

In Fig. 10c (now Fig. 11c), the same open ocean HDRF is used for all illustrated sea ice fractions, while in Fig. 10d (now Fig. 11d), the open ocean HDRF is simulated using the arbitrary parametrization from Eq. 6 (former Eq. 5). Thus, in Fig. 10d (now Fig. 11d), the open ocean HDRF depends on the sea ice fraction, while it doesn't in Fig. 10c (now Fig. 11c). The reconstructed MIZ HDRF, of course, always depends on the sea ice fraction. Obviously, that was not well explained in the original manuscript. Hopefully, it gets more clear in the revised Section (see below).

L358-369 – I don't understand what you want to tell the reader in this paragraph? The measured sunglint HDRF is affected by inhomogeneity of your sparse measurements (as you stated before) and the limitations of your glint masking (which you hardly mention). The simulated ocean HDRF depend on your arbitrary choice of parameterization of effective wind speed in Eq.5. In addition, a better match might be achievable, if you could include smaller effective wind speeds ... leading to even more frequent specular reflection moments. All these uncertainties lead to the fact that you hardly can compare the two HDRF in any detail. Please clarify what your conclusion is. Maybe shorten this part.

With the comparison, we intended to assess the importance of the discrepancies of the open ocean HDRF (homogeneous vs. MIZ) on the constructed HDRF. The conclusion from this comparison is, that the impact of reduced wave intensity at the ocean surface in the MIZ is still obvious even for the constructed HDRF and needs to be considered when constructing a HDRF of the MIZ from individual single-surface HDRFs. We revised and rearranged Sect. 5 completely (see below). Hopefully, our intension is more clear from the revised Section:

In this section, the average HDRF of the inhomogeneous sea ice–open ocean surface in the MIZ is compared to a constructed HDRF of the MIZ assuming a linear combination of the individual HDRFs of open ocean $R_{\mathrm{HDRF,ocean}}$ and sea ice $R_{\mathrm{HDRF,ice}}$ weighted by the sea ice fraction f_{ice}:

(Equation 5)

To do so, the data set was randomly split into two subsets. One of the subsets, the test data set, consists of 35 images (roughly 25 %) that are averaged without separation to obtain a mean HDRF of the inhomogeneous MIZ (mean MIZ HDRF). The sea ice fraction of this dataset was calculated using the sea ice mask. The remaining subset, separation data set, was used to separate and recombine the individual HDRFs to a constructed HDRF. The HDRF histograms of both subsets are shown in Fig. 10. The location of the modes of both data sets is similar to the distribution of the entire dataset (black line). The open ocean mode of the test data set is lower, while its sea ice mode is slightly shifted towards lower values. Nevertheless, the agreement of both data sets suggests, that the same thresholds of the sea ice mask can be applied to all images. The sea ice fraction amounts to 0.83 and 0.81 for the separation and the test data set, respectively, with uncertainties of 4% similar to the complete data set.

The mean MIZ HDRF from the test data set is illustrated in Fig. 11a. Despite the high sea ice fraction, the mean MIZ HDRF shows features both open ocean and sea ice surfaces. The strongly enhanced reflectance in the sunglint region is clearly visible. However, because of the high sea ice fraction, its maximum HDRF (about 3.0) is significantly lower compared to the separated open ocean HDRF (see Fig. 6a). Outside the sunglint but still in forward direction, the slightly enhanced HDRF characteristic for the sea ice surface is imprinted in the mean MIZ HDRF (compare Fig. 8a). For all other directions, the HDRF is more or less isotropic with values slightly lower (mean of 0.76 on the shadow side) than observed in the sea ice HDRF (0.90), due to the contribution of open ocean surfaces.

For comparison, the HDRF of the MIZ is constructed using Eq. 5. Firstly, it is tested if the mean MIZ HDRF from the test data set can be reproduced. The MIZ HDRF is constructed using the separated open ocean and sea ice HDRFs from the separation data set and the sea ice fraction of the test data set (0.81). The constructed HDRF is shown in Fig. 11b and compared to the mean MIZ HDRF (Fig. 11a). The difference between both HDRFs is less than 0.1 for 84% of the pixels. The constructed MIZ HDRF appears more smoothed than the mean MIZ HDRF for statistical reasons. The smoothness was quantified by the standard deviation of the HDRF calculated with respect to all reflection directions of the shadow side (to exclude the sunglint contribution). For the constructed MIZ HDRF the standard deviation is slightly lower (0.03, 4.3% of the mean value) than for the mean MIZ HDRF (0.05, 6.5% of the mean value). The smoothness for the constructed HDRF is due to the assumption a homogeneous and uniform sea ice fraction in Eq. 5, whereas the measured mean HDRF is affected by the directionally inhomogeneous sea ice fraction and the quite low number of images included in the test data set. Figure 12 illustrates the variability of the pixel-based sea ice fraction of the test data set. It is obvious, that for each pixel the pixel-based sea ice fraction is different, covering a wide range between 0.5 and 1.0. Increasing the number of images (which could be reached by, e. g., increasing the sampling frequency, currently 1/6 Hz) would reduce such effects and the pixel-based sea ice fraction would become more homogeneous.

Figures 11c and 11d show cross-sections of the constructed MIZ HDRF along the solar principle plane for different sea ice fractions. In Fig. 11c the individual sea ice and open ocean HDRFs separated from the separation data set are combined for different sea ice fractions. The open ocean and sea ice HDRFs are represented by the sea ice fractions of 0 and 1, respectively. While the HDRF outside the sunglint increases with increasing sea ice fraction, the sunglint contribution decreases without changing its shape. However, as shown in Fig. 7, there is a significant mismatch between the open ocean HDRF in the MIZ and that of the ice-free ocean due to wave attenuation. In Fig. 11c, the constructed HDRF for all sea ice fractions was retrieved using the MIZ open ocean HDRF (sea ice fraction of 0.83). To assess the impact of the surface roughness on the constructed HDRF, in Fi. 11d, $R_{\mathrm{HDRF,ocean}}$ is replaced by a simulated HDRF that depends on the surface roughness

varying with f_{ice}. The simulations are performed in the same way as described in Sect. 4.1 except that the input surface wind speed v_{eff} is parametrized as a linear function of the sea ice fraction:

(Equation 6)

v_{eff} is considered as an effective wind speed, that would produce the same surface roughness and, thus, the same open ocean HDRF if the ocean was ice-free. v_{meas} is the wind speed measured at flight altitude and extrapolated to 10 m altitude. It has to be noted that this very basic relation between surface wind speed and sea ice fraction aims only to illustrate the effects in a qualitative view. Numbers may change if observations for different sea ice conditions are considered. The comparison of Figs. 11c and 11d reveals significant differences in the shape and the position of the sunglint. With decreasing sea ice fraction, the increasing effective wind speed (Eq. 6) causes a shift of the sunglint towards the horizon (compare Fig. 7) in Fig. 11d. Furthermore, the irregular shape and sharp peak visible in Fig. 11c is not present in the smooth simulations. This leads also to a reduced HDRF maximum in Fig. 11d. Nevertheless, the comparison of either of the constructed HDRFs (Figs. 11c or 11d) for the sea ice fraction observed in the test dataset (0.81, purple line) to its mean MIZ HDRF (black line) reveals only small differences outside the sunglint. The HDRF constructed with the simulated open ocean HDRF (Fig. 11d) even shows good agreement to the mean MIZ HDRF at the sunglint slope. In total, the difference between both HDRFs is less than 0.1 for about 82 % of the directions of the solar principle plane.

This analysis has shown that the linear construction of the HDRF from individual HDRFs of open ocean and sea ice is well applicable if the environmental conditions are considered correctly. That also includes the parametrization of the surface roughness of the open ocean (effective surface wind speed), which considerably depends on the sea ice distribution. Neglecting those effects can lead to substantial irregularities in the resulting sunglint position and intensity.

New/updated figures:

Fig. 10: **Same as Fig. 2, but also including the distributions of the separation data set (red) and test data set (blue).**

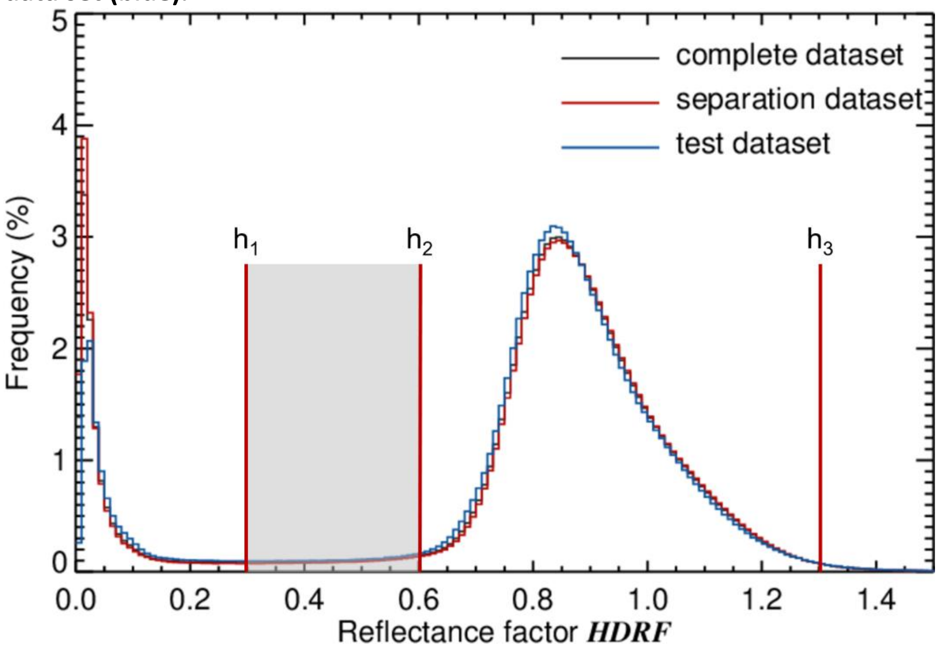

Fig. 11: **Polar plot of (a) the mean MIZ HDRF of the test data set (obtained by averaging over all images without separation), and (b) the constructed MIZ HDRF (calculated from the separated sea ice and open ocean HDRFs of the separation data set according to Eq. 5 using a sea ice fraction of 0.83). (c) Cross-section of the constructed MIZ HDRF along the solar principal plane obtained from the separated HDRFs of the separation data set for different sea ice fractions f_{ice} (color-coded) and the mean MIZ HDRF of the test dataset (black). (d) same as (c), but sea ice fraction-dependent simulations were used for the open ocean HDRF, see text for details.**

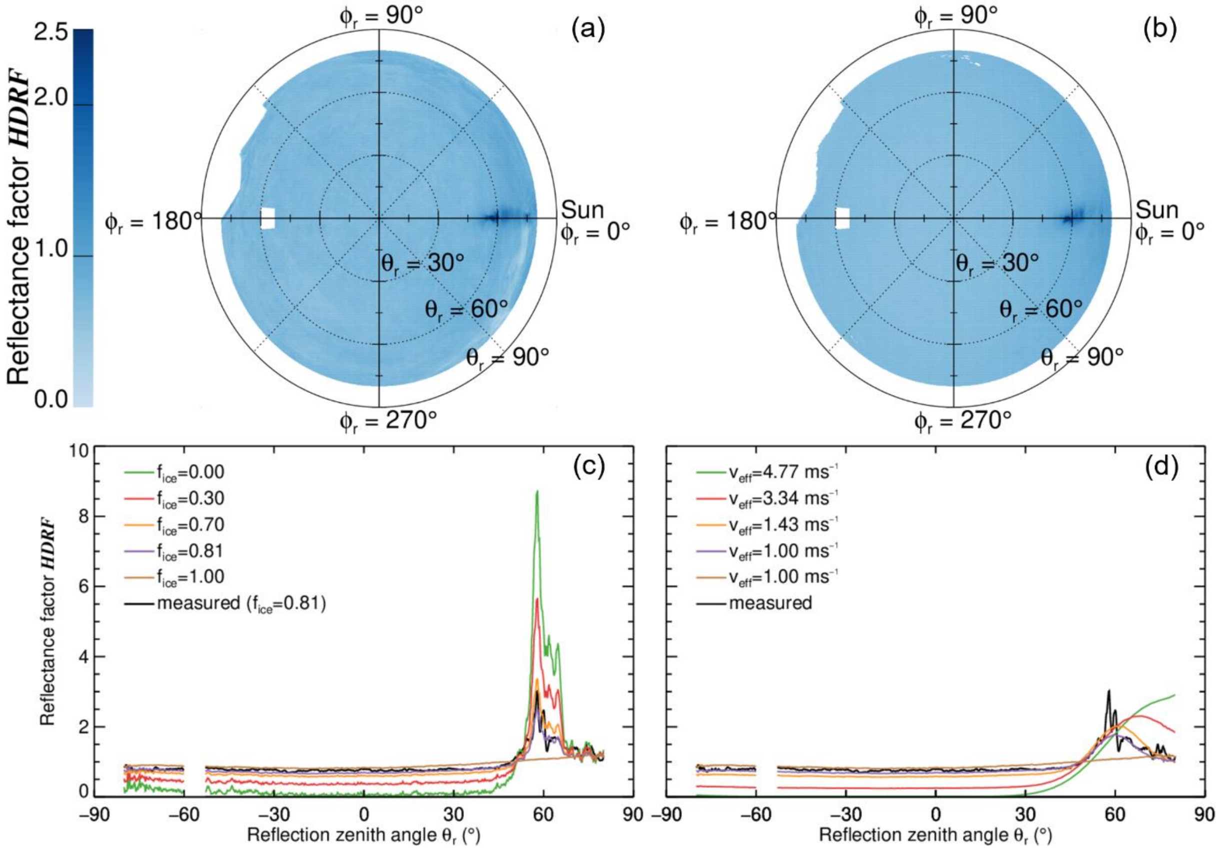

Fig. 12: **Sea ice fraction observed at each pixel throughout the images used for the test sata set (pixel-based sea ice fraction).**

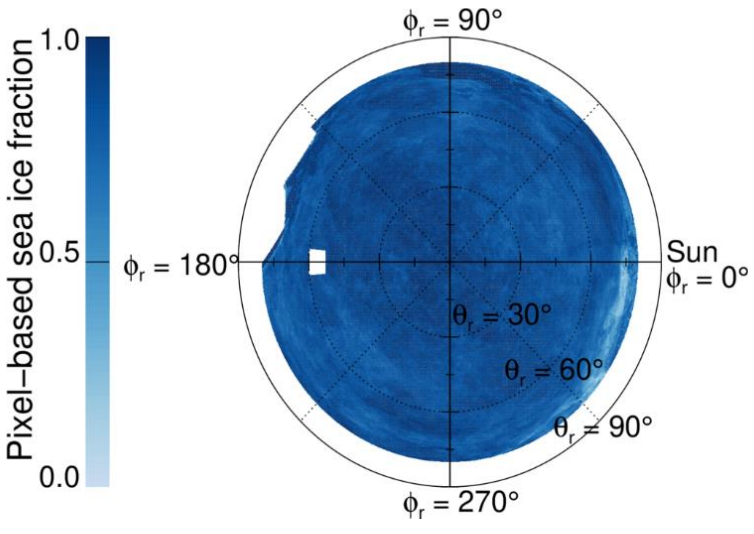

l.382 – "with the irregular distribution of sea ice and open ocean in the MIZ" – and the limitations of your sunglint mask. Please mention.

We changed the sentence to "**The irregular shape of the sunglint observed in the data set was a result of the limitation of the sunglint mask and the highly variable surface roughness associated with the irregular distribution of sea ice and open ocean in the MIZ.**" (l. 401ff)

l.384 – "horizontal photon transport" - Please reference other literature discussing this. It is well known for quite some time that not only local albedo affects the sky brightness. And it is rather not Schaefer et al 2015 who found that first. An older example would be Richiazzi and Gautier 1998, but I'm sure there are others ...

We added the suggested reference "**(e. g., Ricchiazzi and Gautier, 1998; Schäfer et al., 2015)**" (l. 407f).

l.405ff – I'm missing some general outlook what this is good for. What are the limitations of your results? What is needed for it to become a useful method, e.g., for the satellite community (collecting data for different SZA, different wind speeds)? Do you intend to collect such a data set?

The last paragraph of our revised conclusion gives an outlook on further research needed to improve the presented method.

Revised conclusion:

"Reflected radiance measurements were collected by an airborne 180° fish-eye camera in the MIZ north of Svalbard in June 2017. From these data, the HDRF was calculated during cloud-free conditions for a 20-minute sequence of 138 camera images covering different sea ice fractions. The HDRFs of sea ice and open ocean surfaces were separated by applying a sea ice mask with different reflectivity and color ratio thresholds.

From the separated images, the averaged HDRFs of open ocean and snow-covered sea ice surfaces in the MIZ were derived. They confirmed the general features of open ocean and sea ice reported in literature (e. g., Warren et al., 1998; Gatebe et al., 2003; Jackson and Alpers, 2010). However, a comparison with simulations indicated that the common BRDF parametrizations for homogeneous open ocean surfaces as function of the wind speed (Cox and Munk, 1954) partly differ in the MIZ. This is mainly due to wave attenuation between the ice floes in the MIZ (Kohout et al., 2011) leading to a reduced surface roughness compared to a homogeneous open ocean surface with the same surface wind speed. This effect narrows the sunglint and intensifies its magnitude. The irregular shape of the sunglint observed in the data set was a result of the limitation of the sunglint mask and the highly variable surface roughness associated with the irregular distribution of sea ice and open ocean in the MIZ.

The separated HDRF of partly snow-covered sea ice ranged between independent literature HDRFs of homogeneous snow and bare ice surfaces. However, the comparison also revealed the large diverstiy of snow/sea ice HDRF patterns associated with the variability of snow and ice properties. Minor differences between the HDRF in the MIZ and that of homogeneous surfaces could originate

as a result of the radiative effects of the contrasting surface type nearby (e. g., Ricchiazzi et al. 1998, Schäfer et al., 2015).

The averaged HDRF of the MIZ showed features of both sea ice and open ocean surfaces. Even for rather high sea ice fractions, there is still a contribution from the sunglint in the MIZ, which might affect the analysis of satellite observations in these reflection angles. This especially holds regarding the permanent presence of leads in Arctic (e. g., Ivanova et al., 2016).

The mean MIZ HDRF of a subset of the analyzed data set was compared to the constructed one, calculated as a linear combination of the separated HDRFs of the remaining subset weighted by the sea ice fraction. The comparison showed good agreement for the measured sea ice fraction with a difference of less than 0.1 for 84 % of the pixels. Due to the assumption of a directionally constant sea ice fraction, the constructed HDRF of the MIZ was found to be smoother than the mean MIZ HDRF. Altogether, this analysis implies that the construction of the MIZ HDRF from individual sea ice and open ocean HDRFs provides meaningful results. This approach could become relevant for randomly distributed sea ice and open ocean, where only the sea ice fraction is known.

However, the impact of the wave attenuation on the open ocean HDRF in the MIZ has a significant impact also on the sunglint pattern of the MIZ HDRF. This effect needs to be considered in retrieval methods similar to the one used here. To improve the applicability of such methods, further research is needed, regarding the parametrization of the surface roughness of open ocean in the MIZ. Also the impact of the exact floe distribution on the surface reflectance properties needs to be investigated further. To extend the method to different environmental conditions (e. g., sea ice fraction, surface wind speed), further measurements are needed for a full parametrization of the HDRF in such complex scenarios as the MIZ, which may be the dominant surface type of the future Arctic."

Language/ typos:

l.35 – "by about 13 km per decade". Please add "13 km in width".

Actually, that is not necessary. The sentence "**Strong and Rigor (2013) showed that the width of the MIZ increased by about 13 km per decade…**" already indicates that the change refers to the width of the MIZ. (l. 35f)

Fig. 1 caption – "… dots point at …" -> better "…dots label the …" . I had to read the sentence several times, because "dots" and "points" seemed the same word and somehow merged in my mind.

Yes, you are right that this is confusing. We changed it to **"The blue and green dots indicate…"** as suggested by the other referee.

L326: "open open"

The section where this occurred is revised anyway.

L389: “variety” -> “variability”?

We meant “Variety” in the sense of “**diversity**” and changed it accordingly (l. 405).

l.392: “holds” -> “holds true”?

We changed it accordingly (l. 411)